IOP Conf. Series: Journal of Physics: Conf. Series **822** (2017) 012034 doi:10.1088/1742-6596/822/1/012034

Nanofluid heat transfer between concentric independently rotating tubes with axial flow

Mohd Rosdzimin Abdul Rahman[1], Kin Yuen Leong[1], Azam Che Idris[1], Mohd Rashdan Saad[1], Mahmood Anwar[2]

[1]Department of Mechanical, Faculty of Engineering, Universiti Pertahanan Nasional Malaysia, Kem Sg. Besi, 57000, Kuala Lumpur.

[2]Faculty of Engineering and Science, Curtin University, Sarawak Campus, Malaysia

Email: rosdzimin@upnm.edu.my

Abstract. Nanofluid heat transfer behaviour between concentric independently rotating tubes with an axial flow was numerically investigated. Co-rotating and counter-rotating of the inner and outer tubes was simulated at a fixed rotation number. Flow inside the annulus was turbulent with Reynolds number of 5000 and 10000. *k-epsilon* turbulent model was used and the current work is in agreement with published experimental work. Mixture-multiphase model was used to model the multiphase flows of the TiO_2/water nanofluid. Results show that the Nusselt number increases with the Reynolds number. At a constant Reynolds number, different Nusselt number distribution along the hotted tube for co-rotating and counter-rotating tube was observed. The counter-rotating tube was found to be more efficient in enhancing the heat transfer rate in comparison to the co-rotating tube.

1. Introduction

Flows between rotating tubes is known as Taylor-Couette-Poiseuille flow. This type of flow is imminent in industry due to its significant application in rotating machineries and heat exchangers. To optimize the performance of rotating machineries and heat exchangers, a better knowledge of the convective heat transfer is required. The difficulties in carrying out experiments due to higher inner cylinder rotation and narrow gap between the outer and inner cylinders make numerical simulation to be a powerful tool to understand the knowledge of the heat transfer. Poncet *et al*. [1] simulated the heat transfer in rotating tubes and found that the Nusselt number increases with both the rotation rate of the inner cylinder and the Reynolds number. Recently, a study was conducted on an enclosed rotating tube to investigate the stability of the flow submitted to a radial temperature gradient and found that the heat transfer process along the inner and outer walls were enhanced due to the thermo-convective structure of the flow [2].

All the previous investigations on the topic of heat transfer of rotating tubes were only done using water or air. The heat exchanger requires working fluids that possess high thermal conductivity values for a better heat transfer process. Conventional heat transfer fluid such as water and ethylene glycol exhibit low thermal properties. Countless researches have been done to enhance thermal conductivity of conventional fluids by adding nanoparticles. Choi [3] started to add solid particles to increase the thermal conductivity of fluid. Nanometer diameters of the particles were added into the conventional fluid (water, ethylene glycol and oil), which were eventually called nanofluids, showed significant heat transfer enhancement [3]. Many investigations on nanofluids were later done to study the effect of particle type, size, and volume percentage, based on the fluid type and its application in heat exchanger [4-6]. Ting and Hou [6] numerically discovered that the heat transfer coefficient of 2.5 vol % Al_2O_3-water nanofluid increased by 25.5% compared with pure water in force convection case.

The previous studies of nanofluid heat transfer in rotating tubes were focused on forced, natural and mixed convection of the infinite tube length. In the authors' knowledge, no study has been conducted yet on nanofluid heat transfer in finite length independently rotating tubes. Therefore, the objective of the present work is to investigate numerically the heat transfer of TiO_2/water nanofluid in finite length independently rotating tubes.

2. Numerical Works

2.1 Geometry and boundary conditions

Numerical domain of a two-dimensional axi-symmetry tubes with a length of $L/d_h = 60$ and radius ratio ($k = r_1/r_2$) is shown in Fig. 1. A uniform axial velocity is assigned at the velocity inlet based on the Reynolds number. While, a fully developed condition is assumed at the outlet and all derivatives are taken as zero. The inner and outer wall tubes are assigned as a non-slip moving wall condition with N_i and N_o rotation number. A constant heat flux is fixed at the inner tube. The assumptions made for this numerical analysis are; (1) steady state analysis, (2) effective thermo-physical properties of the nanofluid depends on volume concentration, and (3) fluid is continuum.

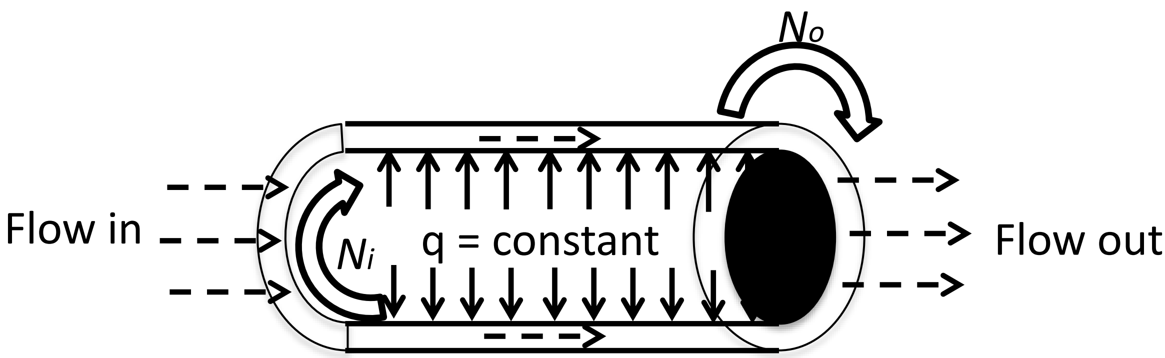

Figure 1. Numerical domain with respective boundary condition.

2.2 Turbulence model

The realizable $\boldsymbol{k-\varepsilon}$ turbulence model was used in this study. Relation of the turbulent viscosity $\boldsymbol{\mu_t = \rho C_\mu k^2/\varepsilon}$ is assigned to combine the turbulent kinetic energy and turbulent dissipation rate.

2.3 Mixture-Multiphase model

The classical mixture theory [7-9] is applied for the Mixture-multiphase model. Generalization principles of continuum mechanics for a single phase to several inter-penetrable continua are employed in this method. Moreover, all phases are assumed to exist at every material point and time in the Mixture model. The Mixture model solves the continuity equation for the mixture, the volume fraction equation for the secondary phase, the momentum equation for the mixture, the energy equation for the mixture and algebraic expressions for the relative velocities.

The continuity equation for the mixture is shown in Eq. 1

$$\boldsymbol{\nabla \cdot (\rho_m \vec{v}_m) = 0} \quad (1)$$

and for the volume fraction of secondary phase is depicted in Eq. 2

$$\nabla \cdot \left(\alpha_p \rho_p \vec{v}_m\right) = -\nabla \cdot \left(\alpha_p \rho_p \vec{v}_{dr,p}\right) \tag{2}$$

Momentum equation

$$\nabla \cdot (\rho_m \vec{v}_m \vec{v}_m) = -\nabla p + \nabla \cdot \left[\mu_m\left(\overrightarrow{\nabla v}_m + \nabla \vec{v}_m^T\right)\right]\dot{m} + \rho_m \vec{g} + \vec{F} + \nabla \cdot \left(\sum_{k=1}^{2} \alpha_k \rho_k \vec{v}_{dr,k} \vec{v}_{dr,k}\right) \tag{3}$$

where$\vec{v}_{dr,k}$ is the drift velocity for secondary phase *k;*

$$\vec{v}_{dr,k} = \vec{v}_k - \vec{v}_m \tag{4}$$

Energy equation is given as

$$\nabla \cdot \sum_{k=1}^{2} (\alpha_k \vec{v}_k (\rho_k E_k + p)) = \nabla \cdot \left(k_{eff} \nabla T\right) + S_E \tag{5}$$

2.4 Numerical procedure
The commercial code Ansys Fluent was employed in the present study. A set of nonlinear partial differential equations was solved by finite volume method. The convergence was set at residual about 10^{-12} for the energy equation.

2.4.1 Validation of the numerical work.
Validation of the Mixture-multiphase model and numerical procedure was done by comparing the axial velocity profile at Reynolds number Re=10000 with the previous experimental work of Rothe and Pfitze [10].

3. Results and discussion
Figure 2 shows a radial distribution of an axial velocity at the outlet of the tubes. It can be seen clearly that the current simulation result is in close agreement with the experimental work by Rothe and Pfitzer [10].

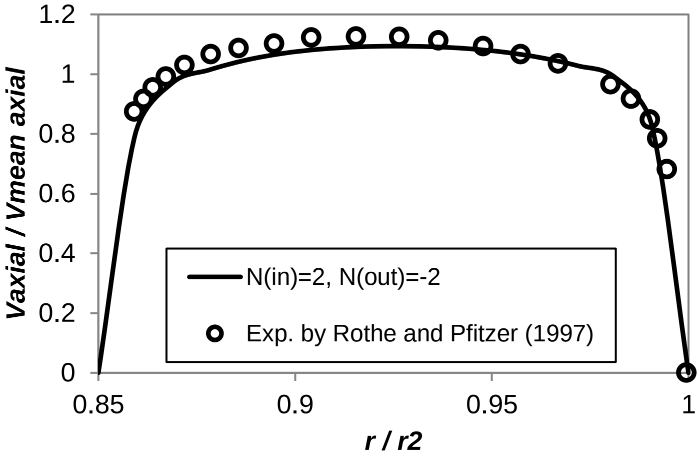

Figure 2. Axial velocity profile for counter-rotating tubes at *Re*=10000.

Figure 3 shows the local Nusselt number along the inner tube wall at Re = 5000 and 10000 for counter-rotating tubes.

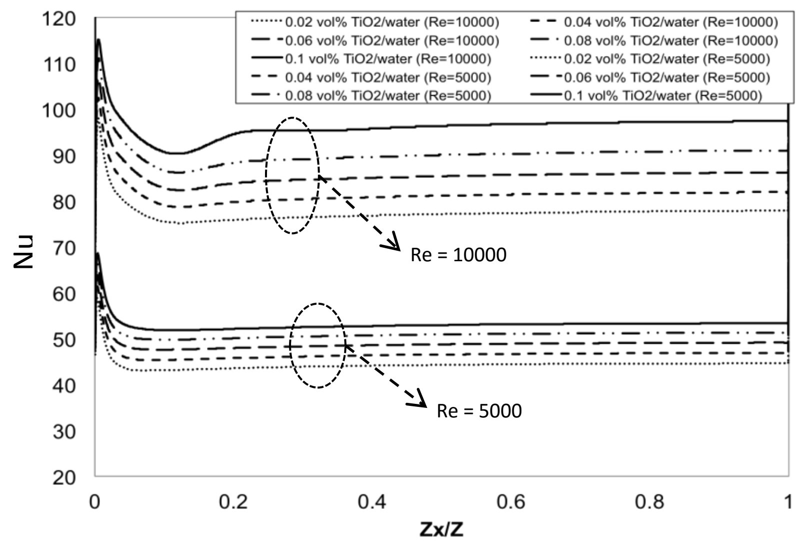

Figure 3. Local Nusselt number along the inner tube wall (N2 N-2) at *Re*= 5000 and 10000.

It can be observed that the Nusselt number is higher at the tube entrance for both cases of Re = 5000 and 10000. The overall recorded Nusselt number for Re=10000 is higher compared to Re = 5000. Moreover, increase in vol% of the TiO_2 nanoparticle contributed to the increase of the Nusselt number. Along the inner tube after the entrance region, the Nusselt numbers recorded were constant for the remaining 80% of the total tube length.

Figure 4 shows the local Nusselt number along the inner tube wall at Re = 5000 and 10000 for co-rotating tubes.

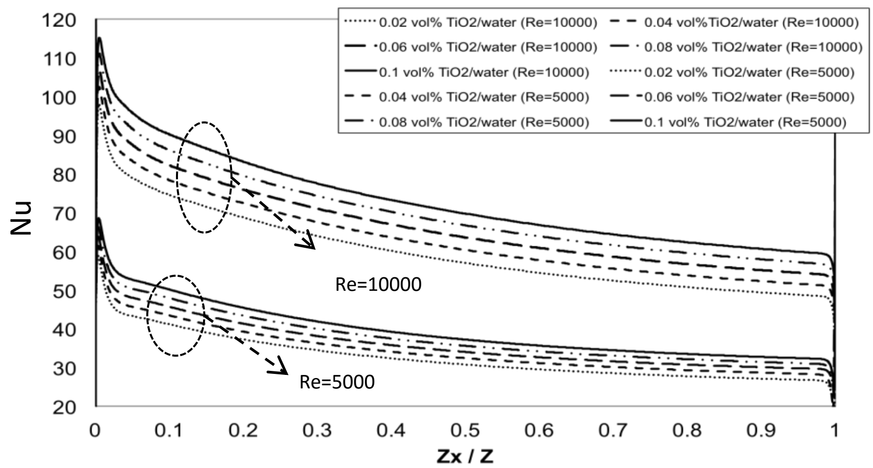

Figure 4. Local Nusselt number along the inner tube wall (N2 N2) at *Re*= 5000 and 10000.

The Nusselt number was found to be higher at the tube entrance for both cases *Re* = 5000 and 10000. The Nusselt number at *Re* = 10000 is higher compared to *Re* = 5000. Moreover, increase in vol% of the TiO_2 nanoparticle also increases the Nusselt number. Along the inner tube, the Nusselt number decreases towards the end of the tube. From the results, it is interesting to discover that the counter-rotating tubes helped significantly to increase the heat transfer compared to co-rotating tubes.

Conclusions

Nanofluid heat transfer behaviour between concentric independently rotating tubes with axial flow was successfully simulated. The Nusselt number for *Re*=5000 and 10000 cases show similarity at the tube entrances for both cases of co-rotating and counter-rotating. Increase in vol% of the TiO_2 nanoparticle increases the Nusselt number. On the other hand, constant Nusselt number is observed along the inner tube for counter-rotating case. The co-rotating case shows a decrease in the Nusselt number towards the tube end. Moreover, the counter-rotating tubes enhanced the heat transfer more effectively compared to the co-rotating tubes for cases of *Re* = 5000 and 10000.

References

[1] Poncet, S., Haddadi, S., Viazzo, S. 2011 *Int. J. Heat Fluid Flow* **32** 128-144
[2] Viazzo S., Poncet S. 2014 *Computer and Fluids* **101** 15-26.
[3] Choi SUS. 1995 Enhancing thermal conductivity of fluids with nanoparticles development and applications of non-newtonian flows, FED-vol. 231/MD-Vol. 66, ASME, New York, (1995) pp 99-105
[4] Alawi O. A., Sidik N. A. C., Mohammed H. A. and Syahrullail S. 2014 *Int. Commun. Heat Mass Transfer*, **56** 50-62.
[5] Leong, K. Y., Nurfadhillah, M. H., Risby M. S. and Hafizah, A. N. 2016 *Therm. Sci.*, **20** 429-436.
[6] Ting, Hsien-Hung and Hou, Shuhn-Shyurng 2015 *Materials*, **8** 5321-5335.
[7] Bowen, R. M., 1976 Theory of Mixtures, Part I. In: Eringen, A. C. (Ed.), Continuum Physics, Vol. III. New York: Academic Press.
[8] Johnson, G., Massoudi, M. &Rajagopal, K. R. 1991, *Chem. Eng. Sci.* **46** 1713 – 1723.
[9] Joseph, D. D., Lundgren, T. S., Jackson, R. &Saville, D. A. 1990 *Int. J. Multiphase Flow* **16** 35 - 42.
[10] Rothe, T., Pfitzer, H. 1997 *Heat and Mass Transfer* **32** 353-364